Magazine of Civil Engineering

ISSN 2712-8172

journal homepage: http://engstroy.spbstu.ru/

DOI: 10.34910/MCE.106.9

Analytical approach to stress-strain analysis of right and oblique helicoid structures

E.M. Tupikova*, M.I. Rynkovskaya

Peoples' friendship university of Russia, Moscow, Russia

**E-mail: emelian-off@yandex.ru*

Keywords: helicoid structure, right helicoid, oblique helicoid, numeric-analytical solution, stress-strain analysis

Abstract. Shell structures with a mid surface of helicoid shape find application in many technical fields, mostly in civil and mechanical engineering. There is a variety of helicoid shells, but the most well-known and used are two types of ruled helicoids: right and oblique. The article is devoted to analytical and numeric-analytical methodologies for shallow right and oblique helicoids. The general approach is based on Kirchhoff–Love linear theory of thin elastic shells. Analytical results can be used for preliminary design and calculations aimed at the understanding of construction physics and regularities of stress-strain state behavior. Two methodologies of stress-strain analysis are presented: the analytical method for shallow right helicoid, and the numeric-analytic method for oblique helicoid (including any special or degenerated case). The numerical results are verified. The results and approach outlined could be of interest to designers and scientists, who want to understand the generalities of thin ruled helicoid shell behavior.

1. Introduction

Shells of helicoidal surface form are permanently in focus among scientists because they have the potential to be applied in the construction [1, 2], architecture [3] and mechanical engineering [4, 5]. The Archimedes screw turbines become popular because of global energy-saving trend [6, 7]. The entrance vehicle and wheelchair ramps are in common use in most objects of urban infrastructure, so the design of such objects is important today. Steel and reinforced concrete helicoid shells of the three most common types – right, oblique and developable, are usually used while designing the objects of different purpose, like parking spaces, transport interchanges, railway junctions, in the most cases the shells are shallow and have small lead of helix. In machine construction, conversely, non-shallow shells of high helix are used. Despite these structures are widely used in very diverse fields [8–12], not so many papers are devoted to mechanics of helicoidal shells and particulary to their stress-strain state [13–17], so the topic seems to be not developed enough. This job is devoted to the design of shallow shells of oblique and right type for structural purposes.

The present study concerns thin elastic shells, which can be calculated in Kirchhoff-Love theoretical model [18]. The models of shells and plates mechanical behaviour are constantly improving, but the Kirchhoff-Love hypothesis remains the basis of the linear elastic shell theory. Such objects have a range of advantages in technical-and-economical indexes, they are light in weight, the minimal thickness of these shells is limited by technological characteristics of erection, like pump-crete machine application. While implementation of special technologies, like concrete pump placing, these limitations can be eliminated.

The research of thin elastic shells has been conducted intensively since the 60-s of 20-s century, the various models and algorithms have been developed [19–22]. All of them can be divided into three main groups: analytical, numeric and numeric analytical methodologies. The right and developable helicoid analyses are more developed comparative to the oblique. Obviously the first two have more simple

Tupikova, E.M., Rynkovskaya, M.I. Analytical approach to stress-strain analysis of right and oblique helicoid structures. Magazine of Civil Engineering. 2021. 106(6). Article No. 10609. DOI: 10.34910/MCE.106.9

expressions of surface equations, and therefore the quadratic forms expressions are simple too. The oblique helicoid equations are defined in general case in non-conjugate non-orthogonal coordinate system, so the expressions are cumbersome.

Among the variety of helicoidal surfaces [23] the most popular and handy are right [24], oblique [25] and developable [26–28] helicoids. At the stage of design study, for comparison and verification of results it is very good to have a standard of reference, some simple example of precise analytical solution that can be used like benchmark before creating detailed complex model. Such an example can be got by analytical approach using modern computer technologies, which give us a powerful software and hardware means of analysis. The analytical methods were popular while designing real objects about 25–30 years ago, and now they are replaced by finite element method. But they are still necessary because of the range of advantages, main of which is obviousness of physical meaning. Due to improvement of both hardware and algorithms, the most of difficulties of computation are resoluble now. If the analytical solution can't be obtained, the equations can be solved by numeric methods. In this case the methodology is called numeric-and-analytic. The accuracy of such methodology is formally lower than the accuracy of analytical methodology and is defined by the numeric method applied, but the results are also valuable [14, 18]. In the present paper analytical and numeric-analytical methods for shallow helicoidal shells are considered for right and oblique helicoids.

2. Methods

2.1. General Methodology

General form of helicoid surface equation can be conceived in vector form:

$$\bar{r}(u,v) = u \cdot \cos(v) \cdot \bar{i} + u \cdot \sin(v) \cdot \bar{j} + (f(u) + c \cdot v) \cdot \bar{k}, \tag{1}$$

Where *c* is a parameter of helix pitch, if $c = 0$ helicoid degenerates into surface of revolution·

If Oz axis is axis of rotation, then $z = f(u)$ is a generator plane curve equation.

The basic terms of surface theory are coefficients or first quadratic form $A,\ B, F,$ which characterize the inner geometry of the surface in any point vicinity, and coefficients of second quadratic forms $M, N,$ which characterize the outer geometry of the surface in any point vicinity [30].

Angle between coordinate lines

$$\chi, \cos\chi = \frac{F}{AB}, \quad \mathrm{tg}\chi = \frac{\sqrt{A^2B^2 - F^2}}{F}, \tag{2}$$

R_u, R_v, R_{uv} are radii of curvature of normal sections along coordinate lines *u* and *v*,

$$\frac{1}{R_v'} = -\frac{N}{B^2}, \frac{1}{R_u'} = -\frac{L}{A^2}, \frac{1}{R_{uv}'} = \frac{M}{AB}, \tag{3}$$

$\bar{u} = u(u,v)$ is a vector of elastic displacement of a point of the middle surface which can be expanded in axis of basic trihedral: $\bar{u} = u_u \frac{\overline{r_u}}{A} + u_v \frac{\overline{r_v}}{B} + u_z \bar{n},$ where u_u, u_v, u_z are displacement components, $\bar{n}$ is normal unit vector.

The Christoffel's symbols of surface coordinates can be expressed in terms of $A,\ B,\ \chi$:

$$\Gamma_{11}^1 = \frac{AB^2 \frac{\partial A}{\partial u} + BA^2 \frac{\partial A}{\partial v} - AB\cos\chi \frac{\partial}{\partial u}(AB\cos\chi)}{A^2B^2 \sin\chi^2}, \tag{4}$$

$$\Gamma_{11}^2 = \frac{-A^2 B\cos\chi\frac{\partial A}{\partial u} + A^2\frac{\partial}{\partial u}(AB\cos\chi) - A^3\frac{\partial A}{\partial v}}{A^2B^2\sin\chi^2},$$

$$\Gamma_{12}^1 = \frac{AB^2\frac{\partial A}{\partial v} - AB^2\cos\chi\frac{\partial B}{\partial u}}{A^2B^2\sin\chi^2},\ \Gamma_{12}^2 = \frac{A^2B\frac{\partial B}{\partial u} - A^2B\cos\chi\frac{\partial B}{\partial u}}{A^2B^2\sin\chi^2},$$

$$\Gamma_{22}^1 = \frac{-AB^2\cos\chi\frac{\partial B}{\partial v} + B^2\frac{\partial}{\partial v}(AB\cos\chi) - A^3\frac{\partial B}{\partial u}}{A^2B^2\sin\chi^2},$$

$$\Gamma_{22}^2 = \frac{A^2B\cos\chi\frac{\partial A}{\partial v} + AB^2\cos\chi\frac{\partial A}{\partial v} - AB\cos\chi\frac{\partial}{\partial v}(AB\cos\chi)}{A^2B^2\sin\chi^2}.$$

While designing shell structure the coordinate system choice is crucial. Among the huge variety of any curvilinear coordinates *u, v* there are some coordinate lines of the important properties, these are: the network of conjugate lines, the network of orthogonal lines, the network of principal curvatures. Any surface can be attributed to curvature lines, which are defined uniquely.

The equations of shell theory can be established in the simplest form if the network of principal curvature is set as coordinate lines of the shell midsurface. The problem is to find analytically curvatures of the surface given. There are some surfaces, which can only be set in curvilinear non-orthogonal non-conjugate coordinate systems.

The classical Kirchhoff-Love thin elastic shell theory is based on the assumptions, the similar to the beam theory. Three-dimensional problem of the theory of elasticity can be reduced to two-dimensional problem because of these assumptions. Stress-strain state of the shell can be presented by functions of two variables, which are coordinates of point on shell midsurface. In this study the non-linear effects are not considered, components of elastic displacement vector and their derivatives are supposed to be so small that the members nonlinear with respect to them, should be neglected.

A.L. Goldenveizer suggested a full system of equations of the thin elastic shell theory, this theory is recognized as a classical [31]. The theory contains several groups of equations: the equilibrium equations, the stress-strain relations, the geometrical relations and continuity equations, (which are not of necessity in the current case). The positive directions of the following inner forces and moments are presented on Fig. 1.

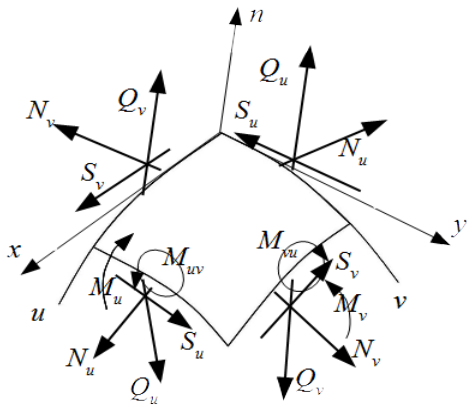

Figure 1.The axis, inner forces and moments.

Equilibrium equations in non-conjugate non-orthogonal (most general type) coordinate system *u, v*:

$$\frac{1}{\sin\chi}\frac{\partial}{\partial u}\left(B\left(N_u + \cos\chi S_u\right)\right) - \frac{B^2}{A}\Gamma_{11}^2\sin\chi S_u - \frac{1}{\sin\chi}\frac{\partial}{\partial v}\left(A\left(S_v - \cos\chi N_v\right)\right) -$$
$$-B\Gamma_{12}^2\sin\chi N_v - \sin\frac{AB}{\chi}\left(\frac{Q_u}{R_u} - \frac{Q_v}{R_{uv}}\right) + AB\left(X + \cos\chi Y\right) = 0 \quad (5)$$

$$\frac{1}{\sin\chi}\frac{\partial}{\partial u}\left(B\left(S_u+\cos\chi N_u\right)\right)-A\Gamma_{12}^{1}\sin\chi N_u+\frac{1}{\sin\chi}\frac{\partial}{\partial v}\left(A\left(N_v-\cos\chi S_v\right)\right)+$$

$$+\frac{A^2}{B}\Gamma_{22}^{1}\sin\chi S_v-\frac{AB}{\sin\chi}\left(\frac{Q_v}{R_v}-\frac{Q_u}{R_{uv}}\right)+AB\left(Y+\cos\chi X\right)=0,$$

$$AB\left(\frac{N_u}{R_u}+\frac{N_v}{R_v}+\frac{S_v-S_u}{R_{uv}}\right)+\frac{\partial}{\partial u}\left(BQ_u\right)+\frac{\partial}{\partial v}\left(AQ_v\right)+AB\sin\chi Z=0,$$

$$\frac{1}{\sin\chi}\frac{\partial}{\partial u}\left(B\left(M_{uv}+\cos\chi M_u\right)\right)-\frac{B^2}{A}\Gamma_{11}^{2}\sin\chi M_u-$$

$$-\frac{1}{\sin\chi}\frac{\partial}{\partial v}\left(A\left(M_v-\cos\chi M_{uv}\right)\right)-B\Gamma_{12}^{2}\sin\chi M_{vu}+ABQ_v=0,$$

$$\frac{1}{\sin\chi}\frac{\partial}{\partial u}\left(B\left(M_u+\cos\chi M_{uv}\right)\right)-A\Gamma_{12}^{1}\sin\chi M_{uv}+$$

$$+\frac{1}{\sin\chi}\frac{\partial}{\partial v}\left(A\left(M_{vu}-\cos\chi M_v\right)\right)+\frac{A^2}{B}\Gamma_{22}^{1}\sin\chi M_v-ABQ_u=0,$$

$$\sin\chi\left(S_u+S_v\right)+\frac{M_{uv}}{R_u}+\frac{M_{vu}}{R_v}+\frac{M_v-M_u}{R_{uv}}=0,$$

where

N_u, N_v are axial forces along *u, v* respectively;

M_u, M_v are bending moments around *u, v* respectively;

$M_{uv}=M_{vu}$ are twisting moments;

Q_u, Q_v are shear forces along *u, v* respectively;

S_u, S_v are cutting forces along *u, v* respectively;

(see Fig. 1)

Strain-displacement relations:

$$\varepsilon_v=\frac{1}{B}\frac{\partial}{\partial v}\left(u_v+u_u\cos\chi\right)-\frac{A\sin\chi^2}{B^2}\Gamma_{22}^{1}u_u+\frac{u_z}{R_v},$$

$$\varepsilon_u=\frac{1}{A}\frac{\partial}{\partial u}\left(u_u+u_v\cos\chi\right)-\frac{B\sin\chi^2}{A^2}\Gamma_{11}^{2}u_v+\frac{u_z}{R_u},$$

$$\omega_u=\frac{\sin\chi}{A}\frac{\partial}{\partial u}u_v-\left(\frac{\sin\chi}{B}\Gamma_{12}^{1}+\frac{1}{A}\frac{\partial\chi}{\partial v}\right)u_u+$$

$$+\cos\chi\left(\frac{B\sin\chi}{A^2}\Gamma_{11}^{2}+\frac{1}{A}\frac{\partial\chi}{\partial u}\right)u_v-\frac{1}{\sin\chi}\left(\frac{1}{R_{uv}}+\frac{\cos\chi}{R_u}\right)u_z,$$

(6)

$$\omega_v = \frac{\sin\chi}{B}\frac{\partial}{\partial v}u_u - \left(\frac{\sin\chi}{B}\Gamma_{12}^2 + \frac{1}{B}\frac{\partial\chi}{\partial v}\right)u_v +$$

$$+\cos\chi\left(\frac{A\sin\chi}{B^2}\Gamma_{22}^1 + \frac{1}{B}\frac{\partial\chi}{\partial v}\right)u_u - -\frac{1}{\sin\chi}\left(\frac{1}{R_{uv}} + \frac{\cos\chi}{R_v}\right)u_z,$$

$$\varepsilon_{uv} = \omega = \omega_u + \omega_v,$$

$$\gamma_u = \frac{1}{A}\frac{\partial}{\partial u}u_z - \frac{u_u}{R_u} + \frac{u_v}{R_{uv}},\ \delta = \frac{1}{2}\left(\omega_v - \omega_u\right),$$

$$\kappa_u = -\frac{1}{A}\frac{\partial}{\partial u}\left(\frac{\gamma_u - \gamma_v\cos\chi}{\sin\chi}\right) - \frac{\sin\chi}{B}\Gamma_{12}^1\gamma_v + \frac{\delta}{R_{uv}},$$

$$\kappa_v = -\frac{1}{B}\frac{\partial}{\partial v}\left(\frac{\gamma_v - \gamma_u\cos\chi}{\sin\chi}\right) - \frac{\sin\chi}{A}\Gamma_{12}^2\gamma_u - \frac{\delta}{R_{uv}},$$

$$\tau^{(1)} = -\frac{1}{A}\frac{\partial}{\partial u}\left(\frac{\gamma_v - \gamma_u\cos\chi}{\sin\chi}\right) - \frac{B\sin\chi}{A^2}\Gamma_{11}^2\gamma_u + \frac{\delta}{R_u},$$

$$\tau^{(2)} = -\frac{1}{A}\frac{\partial}{\partial v}\left(\frac{\gamma_u - \gamma_v\cos\chi}{\sin\chi}\right) - \frac{A\sin\chi}{B^2}\Gamma_{22}^1\gamma_u + \frac{\delta}{R_u},$$

$$\tau^{(1)} = \kappa_{uv} - \kappa_u\cos\chi + \frac{1}{R_{uv}}\left(\varepsilon_v\sin\chi - \frac{\varepsilon_{uv}\cos\chi}{2}\right) - \frac{\varepsilon_{uv}}{2R_u},$$

$$\tau^{(2)} = -\kappa_{uv} + \kappa_v\cos\chi - \frac{1}{R_{uv}}\left(\varepsilon_u\sin\chi - \frac{\varepsilon_{uv}\cos\chi}{2}\right) - \frac{\varepsilon_{uv}}{2R_v},$$

where ε_u is relative tension of middle surface along line *u*;

ε_v is relative tension of middle surface along line *v*;

ε_{uv} is alteration of angle between lines *u*, *v*;

γ_u is angle of rotation of vector $\bar{r}_u$ towards vector *n* in plane $\left(\bar{r}u, n\right)$;

γ_v is angle of rotation of vector $\bar{r}_v$ towards vector *n* in plane $\left(\bar{r}_v, n\right)$;

ω_u is angle of rotation of vector $\bar{r}_u$ towards vector $\bar{r}_v$ in tangent plane;

ω_v is angle of rotation of vector $\bar{r}_v$ towards vector $\bar{r}_u$ in tangent plane;

Γ_{ij}^n are Christoffel's symbols (with 3 indexes).

The two subscripts specify derivative variables for $\bar{r} = u\left(u, v\right)$ on the left side of the corresponding equality, and the superscript indicates which derivative of $\bar{r} = u\left(u, v\right)$ is followed by this coefficient (the digit 1 corresponds to the parameter *u*, and the digit 2 corresponds to the parameter *v*).

The stress-strain (physical) relations in accordance with Hooke's law:

$$N_u = \frac{Eh}{\left(1-\nu^2\right)}\left(\frac{\varepsilon_u - \varepsilon_{uv}\mathrm{ctg}\chi + \nu\varepsilon_v}{\sin\chi}\right),\ N_v = \frac{Eh}{\left(1-\nu^2\right)}\left(\frac{\varepsilon_v - \varepsilon_{uv}\mathrm{ctg}\chi + \nu\varepsilon_u}{\sin\chi}\right),$$

$$S_u = -S_v = \frac{Eh}{2\left(1-\nu^2\right)}\left(\frac{1+\cos^2\chi}{\sin^2\chi}\varepsilon_{uv} - \left(\varepsilon_u - \varepsilon_v\right)\mathrm{ctg}\chi\right) - \frac{Eh}{2\left(1-\nu^2\right)}\nu\left(\varepsilon_{uv} - \left(\varepsilon_u - \varepsilon_v\right)\mathrm{ctg}\chi\right), \quad (7)$$

$$M_u = -\frac{Eh^3}{12\left(1-\nu^2\right)}\left(\frac{\kappa_u + \nu\kappa_v}{\sin\chi}\right),\ M_v = -\frac{Eh^3}{12\left(1-\nu^2\right)}\left(\frac{\kappa_v + \nu\kappa_u}{\sin\chi}\right),$$

$$M_{uv} = \frac{Eh^3}{12\left(1+\nu\right)}\left(\frac{\kappa_{uv} - \cos\chi\kappa_v}{\sin\chi}\right),\ M_{vu} = -\frac{Eh^3}{12\left(1+\nu\right)}\left(\frac{\kappa_{uv} + \cos\chi\kappa_u}{\sin\chi}\right),$$

Where E is modulus of elasticity, h is shell thickness, ν is Poisson's ratio.

These expressions form the system of 20 design equations, which makes possible to define two-dimensional parameters of inner forces and moments.

2.2. Oblique helicoid stress-strain analysis

2.2.1 Theoretical base

The oblique helicoid is a surface arising by moving oblique line along helicoidal line (Fig. 2). The much-used parametrical equation of this surface can be conceived of as [28]:

$$x = u\cdot\cos\left(v\right),\ y = u\cdot\sin\left(v\right),\ z = k\cdot u + c\cdot v, \quad (8)$$

where k is generator's slope ratio.

This is the equation in cylindrical coordinate system (Fig. 2, a). Also the oblique helicoid surface equations (5) can be established in oblique axis (Fig. 2, b):

$$x = u\cdot\cos\left(\varphi\right)\cdot\cos\left(v\right),\ y = u\cdot\cos\left(\varphi\right)\cdot\sin\left(v\right),\ z = u\cdot\sin\left(\varphi\right) + c\cdot v, \quad (9)$$

v coordinate is generator rotation angle, like in cylindrical system, $\varphi = const$ is the generator obliquity angle.

This coordinate system is non-orthogonal and non-conjugate, but the expressions of quadratic forms would be slightly simpler in comparison to those in cylindrical system:

$$A = 1, B = \sqrt{u^2\cdot\cos^2\varphi + c^2},\ F = c\cdot\sin\varphi,$$

$$M = -\frac{c\cdot\cos\varphi}{\sqrt{u^2+c^2}},\ N = -\frac{u^2\cdot\sin 2\varphi}{\sqrt{u^2+c^2}},\ \chi = a\cdot\cos\pm\left(\frac{c\cdot\sin\varphi}{\sqrt{u^2\cdot\cos^2\varphi + c^2}}\right). \quad (10)$$

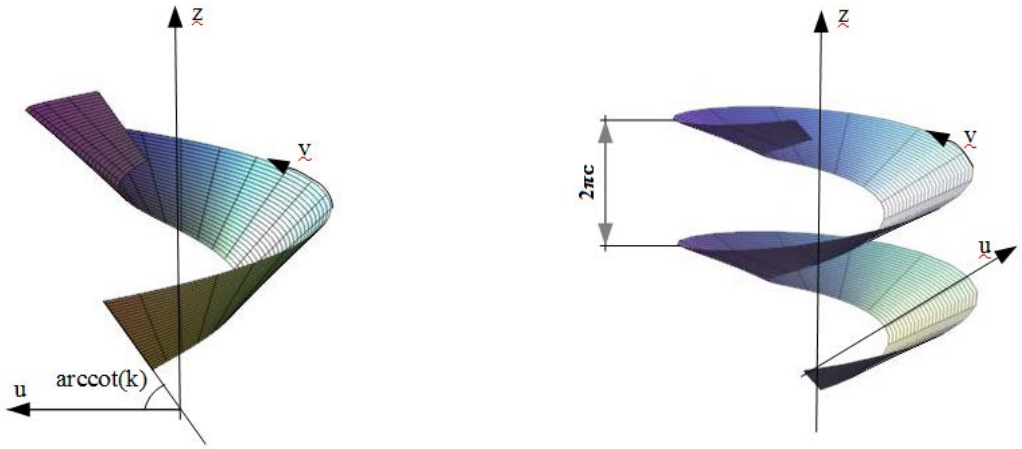

a) In cylindrical coordinate system **b) In curvilinear coordinate system**

Figure 2. Oblique helicoids.

To simplify the task, assume that the helicoid has many coils, and the stress-strain state does not depend on the boundary conditions along the straight borders, and, consequently, does not depend on *v* coordinate.

The methodology is well known in shells and plates theory, it is quite straightforward, like brute-force solution. Substituting the strain-displacement relations (6) into the stress-strain equations (7), and after that the forces and moments expressions into the equilibrium equations (5), finally we can obtain a system of 3 ordinary differential equations in displacements. Actually, all parameters are expressed by displacements to get rid of other unknown variables, except three displacements and their derivatives. The main computational problem is to obtain and simplify the coefficients before them, because they are quite cumbersome. The full system of equations is not quoted in this article because of excessive volume, all procedure of dealing with those cumbersome coefficients and their's simplification is computerized. Modern smart software provides an opportunity to process huge symbolic expressions and exclude mistakes of "human element".

The general form of the differential equation system is given below:

$$\begin{aligned}
\frac{d^2u_u}{du^2} &= K_{10}u_u + K_{11}\frac{du_u}{du} + K_{12}u_v + K_{13}\frac{du_v}{du} + K_{14}u_z + K_{15}\frac{du_z}{du} + K_{16}\frac{du_z}{du} + K_{17}\frac{d^2u_u}{du^2} + K_{1X}X,\\
\frac{d^2u_v}{du^2} &= K_{30}u_u + K_{31}\frac{du_u}{du} + K_{32}u_v + K_{33}\frac{du_v}{du} + K_{34}u_z + K_{35}\frac{du_z}{du} + K_{36}\frac{du_z}{du} + K_{37}\frac{d^2u_u}{du^2} + K_{3Y}Y,\\
\frac{d^4u_z}{du^4} &= K_{70}u_u + K_{71}\frac{du_u}{du} + K_{72}u_v + K_{73}\frac{du_v}{du} + K_{74}u_z + K_{75}\frac{du_z}{du} + K_{76}\frac{du_z}{du} + K_{77}\frac{d^2u_u}{du^2} + K_{7Z}Z.
\end{aligned} \quad (11)$$

The system can be reduced into the first-order system of 8 differential equations by the substitution:

$$u_u = y_0,\ \frac{du_u}{du} = y_1,\ u_v = y_2,\ \frac{du_v}{du} = y_3,\ u_z = y_4,\ \frac{du_z}{du} = y_5,\ \frac{d^2u_z}{du^2} = y_6,\ \frac{d^3u_z}{du^3} = y_7. \quad (12)$$

This is a routine procedure of reduction of order of ordinary differential equation system.

Finally, we can obtain the first-order system of ordinary differential equations $\frac{dy}{dx} = f(x, y)$, or in other terms $y' = f(x, y)$ where:

$$y=\begin{bmatrix} y_0 \\ y_1 \\ y_2 \\ y_3 \\ y_4 \\ y_5 \\ y_6 \\ y_7 \end{bmatrix}=\begin{bmatrix} u_u \\ (u_u)' \\ u_v \\ (u_v)' \\ u_z \\ (u_z)' \\ (u_z)'' \\ (u_z)''' \end{bmatrix},\ f(u,y_i)=\begin{bmatrix} f_0 \\ f_1 \\ f_2 \\ f_3 \\ f_4 \\ f_5 \\ f_6 \\ f_7 \end{bmatrix}=\begin{bmatrix} y_1 \\ f_1 \\ y_3 \\ f_3 \\ y_5 \\ y_6 \\ y_7 \\ f_7 \end{bmatrix}=\begin{bmatrix} (u_u)' \\ (u_u)'' \\ (u_v)' \\ (u_v)'' \\ (u_z)' \\ (u_z)'' \\ (u_z)''' \\ (u_z)'''' \end{bmatrix}, \quad (13)$$

$$f_1=k_{10}y_0+k_{11}y_1+k_{12}y_2+k_{13}y_3+k_{14}y_4+k_{15}y_5+k_{16}y_6+k_{17}y_7,$$

$$f_3=k_{30}y_0+k_{31}y_1+k_{32}y_2+k_{33}y_3+k_{34}y_4+k_{35}y_5+k_{36}y_6+k_{37}y_7,$$

$$f_7=k_{70}y_0+k_{71}y_1+k_{72}y_2+k_{73}y_3+k_{74}y_4+k_{75}y_5+k_{76}y_6+k_{77}y_7.$$

The full system of 8 differential equations is not presented in the article because of excessive volume.

The boundary conditions were considered as that: The shell was fixed rigidly along the whole contour. Its calculation model's boundary conditions with this support were supplemented by conditions: $u_u(u_1)=u_v(u_1)=u_z(u_1)=u_z'(u_1)=0, u_u(u_2)=u_v(u_2)=u_z(u_2)=u_z'(u_2)=0,$ where u_1 and u_2 are the coordinates of inner and outer curvilinear edges.

These ordinary differential equation systems can be solved by numeric methods [32, 33], particularly by means of sweep method, which is constantly improving and being modified [34, 35]. Differential sweep method of the most simple modification let solve such systems in case of the most simple boundary conditions, that is demonstrated in the present job. Through the sweep method algorithm execution the corresponding Cauchy's problems are solved by Runge-Kutta-Fehlberg 5'th order method, that is realized by Giac/Xcas software package for symbolic calculations. In prospect of this job, modified methods of orthogonal successive substitution will make possible to solve similar systems with more complex boundary conditions ensuring the calculation stability.

So that, this method can be called numeric-analythical or semi-analythical, because the faithful and obvious in their physical meaning differential equations are solved by approximate numeric method. With some initial modifications and assumptions the methodology can be applied to shallow or non-shallow shells (the non-shallow variant is more universal, but demands more resources of computer). In the present article the modification for shallow shells was applied.

After calculating the deformations and their derivatives we can calculate internal axial and shear forces and bending and twisting moments.

2.2.2 Numeric experiments

Modern computers and software have high potential for either numerical or symbolic computations, and provide wide opportunities for processing cumbersome expressions. Thus, computational complexities, like stress-strain analysis of thin shells in non-orthogonal non-conjugate system, can be fulfilled and realized. The series of numeric experiments were conducted for helicoidal shells with variable geometrical parameters. Both shallow and non-shallow shells were investigated. In the first series of numeric experiments the influence of the generator obliquity angle on the stress-strain state was analyzed.

The series of numeric experiments were conducted for helicoidal shells with variable geometrical parameters. In the present job the shallow shells were investigated.

The calculation example for the methodology is given for the shell of reinforced concrete material

(Fig. 3). Both edges are fixed, an equally distributed vertical load is applied. The generators obliquity angle φ = 5°, contour radius R_1 = 2 m, R_2 = 4 m; thickness of 12 cm and pitch of 0.01·2π. The material characteristics: modulus of elasticity E = 32500 MPa, Poisson's ratio v = 0.17. Load intensity is 10 kPa (Fig. 4). The approach is performed by Giac/Xcas software. The test results are shown in Fig. 5.

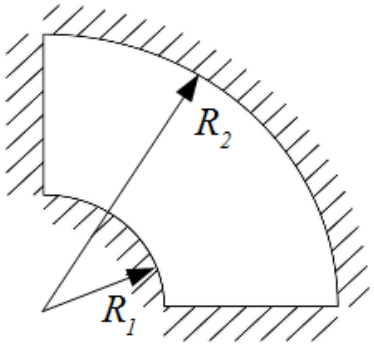

Figure 3. The model scheme.

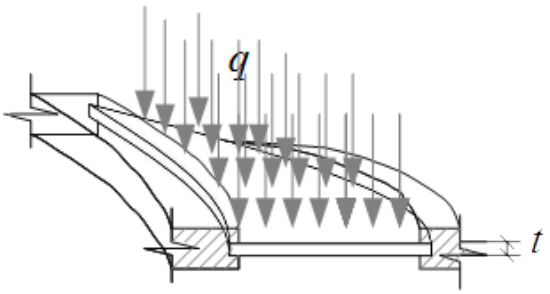

Figure 4. The loading.

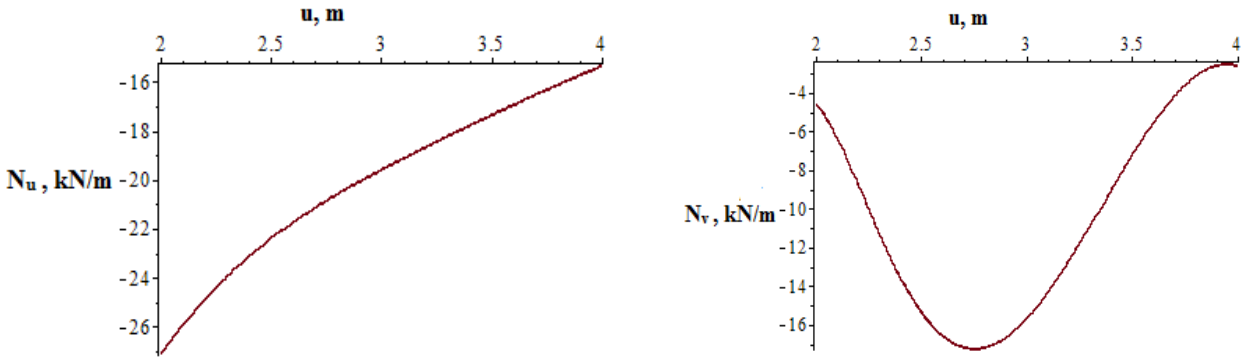

Figure 5. Inner axial forces.

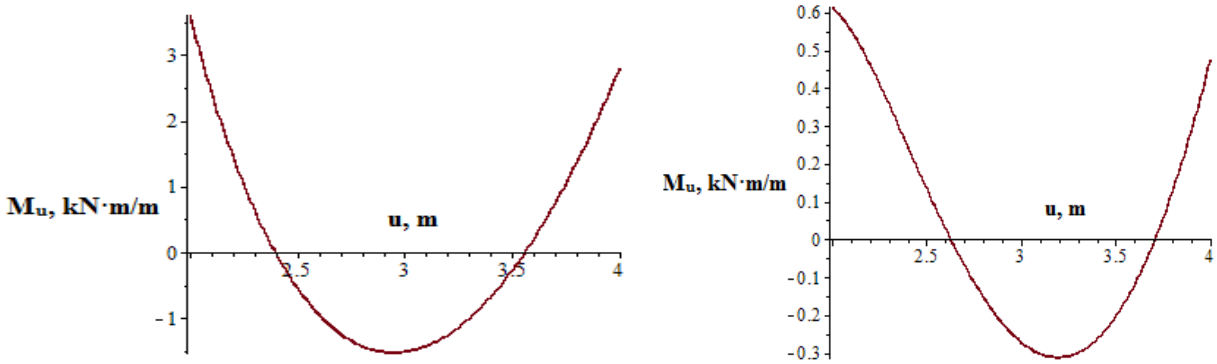

Figure 6. Inner bending moments.

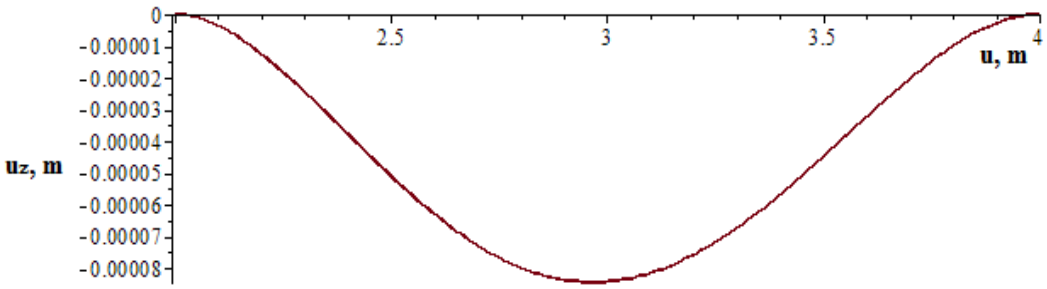

Figure 7. Deflection.

2.3. Right helicoid stress-strain analysis

The right helicoid (Fig. 5) is a surface arising by moving a straight line along helicoidal line when the angle between the straight line and the axis of the surface is equal to 90º. The much-used parametrical equation of this surface can be conceived of as:

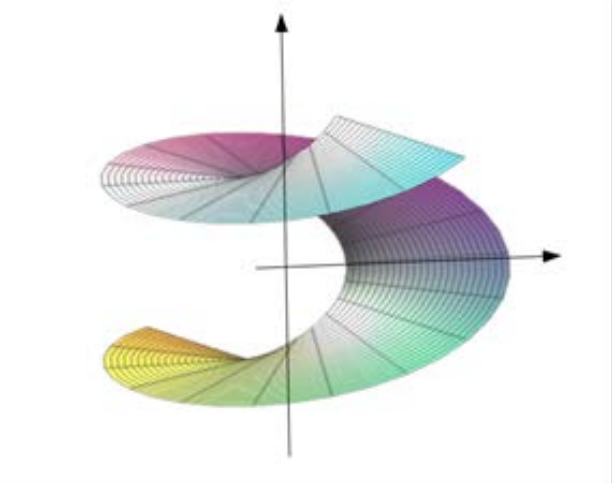

Figure 8. Right helicoid.

$$x = u\cos v\sqrt{b^2 - 4ac}\ ,\ y = u\sin v\ ,\ z = cv\ , \tag{14}$$

where c is displacement of the generator upon its rotation by 1 radian, or the ratio of the translational velocity to the circular velocity;

u, v are curvilinear coordinates of the point C of helicoids;

u is the distance from point C to axis z;

v is the rotation angle of generator AB from the plane zOx to the point C.

For right helicoids $f(u) = 0$ and coefficients of the first and second quadratic forms are

$$A^2 = 1,\ B^2 = u^2 + c^2,\ F = 0,\ \chi = \pi/2,\ \cos\chi = 0,$$

$$L = 0,\ M = -c\Big/\sqrt{u^2 + c^2}\ ,\ N = 0.$$

If input the first and second quadratic form coefficients into

$$\begin{vmatrix} A^2du + Fdv & Fdu + B^2dv \\ Ldu + Mdv & Mdu + Ndv \end{vmatrix} = 0$$

It can be found

$$du^2 = \left(u^2 + c^2\right)dv^2, \tag{15}$$

$$du\Big/dv = \pm\sqrt{u^2 + c^2}\ ,.$$

The angle between direction du/dv and direction $dv = 0$ is α,

$$\cos\alpha = \frac{A^2du + Fdv}{\sqrt{A^2du^2 + 2Fdudv + B^2dv^2}} = \frac{du}{\sqrt{du^2 + \left(u^2 + c^2\right)dv^2}}\ du\ \Big/\sqrt{2du^2} = \sqrt{2}/2 \tag{16}$$

It means that the angle between every direction and generator $dv = 0$ is 45º.

Main curvatures may be found by the equation

$$\lambda = \frac{1}{R} = \frac{Ldu + Mdv}{A^2 du + Fdv}$$

and for the right helicoid

$$\frac{1}{R_{1,2}} = \mp \frac{c}{u^2 + c^2},\ k = k_1 k_2 = -\frac{c^2}{\left(u^2 + c^2\right)^2},\ k_{cp} = 0. \tag{17}$$

The third equation of (17) shows that right helicoid is a minimal surface, the second equation of (17) shows that the torsion of a helical line passing through a given point of a straight helicoid can be expressed by quantity $\sqrt{-k} = \frac{c}{u^2 + c^2}$.

Shell is considered to be shallow if the following conditions are satisfied: $\frac{l_{\min}}{f} \geq 5, \frac{R_{\min}}{h} \geq 20$.

Where $l_{\min}$ is minimum size of the shell projection f is shell depth, h is shell thickness, $R_{\min}$ is minimum radius.

For shallow shells equilibrium equations can be reduced, and geometrical and physical relations can be essentially simplified. After the transformations finally one equation from equilibrium group and one equation of continuity base the system of mixed-mode method.

Differential operators

$$\nabla^2 ... = \frac{1}{\sqrt{u^2 + c^2}} \left[\frac{\partial}{\partial u} \left(\sqrt{u^2 + c^2}\, \frac{\partial ...}{\partial u} \right) + \frac{1}{\sqrt{u^2 + c^2}} \frac{\partial^2 ...}{\partial v^2} \right],$$

$$\nabla_k^2 ... = -\frac{2c}{\left(u^2 + c^2\right)^{3/2}} \frac{\partial}{\partial v} \left(\frac{\partial ...}{\partial u} - \frac{u ...}{u^2 + c^2} \right). \tag{18}$$

In the case of shallow helicoid analysis c^2 can be neglected in comparison to u^2, and the first and second quadratic forms coefficients will be:

$$A = 1,\ B = u,\ F = 0,\ L = 0,\ M = -c/u,\ N = 0,$$

$$\nabla^2 ... = \frac{1}{u} \left[\frac{\partial}{\partial u} \left(u \frac{\partial ...}{\partial u} \right) + \frac{1}{u} \frac{\partial^2 ...}{\partial v^2} \right], \tag{19}$$

$$\nabla_k^2 ... = -\frac{2c}{u^2} \frac{\partial}{\partial u} \left(\frac{1}{u} \frac{\partial ...}{\partial v} \right) = -\frac{H}{\pi} \frac{1}{u^2} \frac{\partial}{\partial u} \left(\frac{1}{u} \frac{\partial ...}{\partial v} \right),$$

where $H = 2\pi c$. The calculation equations for the shallow helical shells:

$$\nabla^2 \nabla^2 \varphi = -E \cdot h \cdot \frac{H}{\pi} \cdot \frac{1}{r^2} \cdot \frac{\partial}{\partial r} \left(\frac{1}{r} \frac{\partial u_z}{\partial v} \right), \tag{20}$$

$$\nabla^2\nabla^2\varphi = -E\cdot h\cdot\frac{H}{\pi}\cdot\frac{1}{r^2}\cdot\frac{\partial}{\partial r}\left(\frac{1}{r}\frac{\partial u_z}{\partial v}\right),$$

which were derived by E. Reissner on the basis of K. Markever's equations for round plates having large deformations. They are solved for a number of particular cases $u_z = u_z(u)$ and $\phi = \phi(u), u_z = kv$ and some others. V.G. Rekach and S.N. Krivoshapko proposed more general cases of solving equations (20). The methodology was developed in [23] and some numeric results were obtained.

Equations (20) are equations of Eulerian type and are reduced to equations with constant coefficients by substitution

$$u = e^t \text{ or } t = \ln u .$$

While using the following relations

$$\frac{d...}{du} = \frac{1}{u}\frac{d...}{dt},$$

$$\frac{d^2...}{du^2} = \frac{1}{u^2}\left(\frac{d^2...}{dt^2} - \frac{d...}{dt}\right),$$

$$\frac{d^3...}{du^3} = \frac{1}{u^3}\left(\frac{d^3...}{dt^3} - 3\frac{d^2...}{dt^2} + 2\frac{d...}{dt}\right), \quad (21)$$

$$\frac{d^4...}{du^4} = \frac{1}{u^4}\left(\frac{d^4...}{dt^4} - 6\frac{d^3...}{dt^3} + 11\frac{d^2...}{dt^2} - 6\frac{d...}{dt}\right),$$

Homogenous operators can be obtained:

$$\nabla^2... = \frac{1}{u^2}\left(\frac{\partial^2...}{\partial t^2} + \frac{\partial^2...}{\partial v^2}\right),$$

$$\nabla^4... = \frac{1}{u^4}\left(\frac{\partial^4...}{\partial t^4} - 4\frac{\partial^3...}{\partial t^3} + 4\frac{\partial^2...}{\partial t^2} - 4\frac{\partial^3...}{\partial t\partial v^2} + 2\frac{\partial^4...}{\partial t^2\partial v^2} + 4\frac{\partial^2...}{\partial v^2} + \frac{\partial^4...}{\partial v^4}\right), \quad (22)$$

$$\nabla_k^2... = \frac{1}{u^4}\frac{\partial}{\partial v}\left(\frac{\partial}{\partial t^2} - 1\right)...,$$

If switching from coordinates u, v to u, t the (20) will become:

$$\nabla^4(t,v)u_z - \frac{H}{\pi D}\nabla_k^2(t,v)\phi = e^{4t}\frac{Z}{D},$$

$$\nabla^4(t,v)\phi + \frac{EhH}{\pi}\nabla_k^2(t,v)u_z = 0, \quad (23)$$

where $\nabla^4(t,v)... = u^4\nabla^4...,\ \nabla_k{}^4(t,v)... = u^4\nabla_k{}^4...,$

In the case of determination: $\phi = \left(\frac{EhH}{\pi}\right)\nabla_k^2(t,v)\Phi(t,v)$, and $u_z = -\nabla^4(t,v)\Phi(t,v)$ equations (17) can be combined into one equation of eight order:

$$\nabla^8(t,v)\Phi(t,v) + p^2\nabla_k^4(t,v)\Phi(t,v) = -e^{4t}Z(t,v)/D, \quad (24)$$

where $p^2 = \frac{EhH^2}{\pi^2 D} = \frac{12\left(1-\nu^2\right)H^2}{\pi^2 h^2}$.

The solution of equation (24) can be found in trigonometric Fourier series

$\Phi(t,v) = \sum_{m=1}^{\infty} \Phi_m(t)\sin mv$ where coefficients of the series may be obtained from differential equations

$$\nabla^8(t,m)\Phi(t) - p^2\nabla_k^4(t,m)\Phi(t) = 0,$$

where $p^2 = \frac{EhH^2}{\pi^2 D} = \frac{12\left(1-\nu^2\right)H^2}{\pi^2 h^2}$.

$$\nabla^4(t,m)... = \frac{d^4...}{dt^4} - 4\frac{d^3...}{dt^3} + 2\left(2-m^2\right)\frac{d^2...}{dt^2} + 4m^2\frac{d...}{dt} + m^2\left(m^2-4\right)...$$
$$\nabla_k^2(t,m)... = \pm m\left(\frac{d}{dt} - 1\right)...\cdot \quad (25)$$

In this case inner forces and moments are obtained from the following formulas:

$$N_u = \frac{1}{u}\frac{\partial\phi}{\partial u} + \frac{1}{u^2}\frac{\partial^2\phi}{\partial v^2} = \pm\frac{EhH}{\pi}\frac{1}{u}\sum_{m=1}^{\infty}\left(\frac{d}{du} - \frac{m^2}{u}\right)\nabla_k^2(u,m)\Phi_m(u)\sin mv,$$

$$N_v = \frac{\partial^2\phi}{\partial u^2} = \pm\frac{EhH}{\pi}\frac{d^2}{du^2}\sum_{m=1}^{\infty}\nabla_k^2(u,m)\Phi_m(u)\sin mv,$$

$$S = -\frac{\partial}{\partial u}\left(\frac{1}{u}\frac{\partial\phi}{\partial v}\right) = \frac{EhH}{\pi}\frac{1}{u}\left(\frac{d}{du} - \frac{1}{u}\right)\sum_{m=1}^{\infty} m\nabla_k^2(u,m)\Phi_m(u)\sin mv,$$

$$Q_u = -D\frac{\partial}{\partial u}\nabla^2 u_z = D\frac{d}{du}\frac{1}{u^2}\sum_{m=1}^{\infty}\nabla^6(u,m)\Phi_m(u)\sin mv,$$

$$Q_v = -\frac{D}{u}\frac{\partial}{\partial v}\nabla^2 u_z = \pm\frac{D}{u^3}\sum_{m=1}^{\infty} m\nabla^6(u,m)\Phi_m(u)\sin mv, \quad (26)$$

$$M_u = -D\left[\frac{\partial^2 u_z}{\partial u^2} + \frac{\nu}{u}\left(\frac{\partial u_z}{\partial u} + \frac{1}{u}\frac{\partial^2 u_z}{\partial v^2}\right)\right] =$$

$$= D\sum_{m=1}^{\infty}\left[\frac{d^2}{du^2} + \frac{\nu}{u}\left(\frac{d}{du} - \frac{m^2}{u}\right)\right]\nabla^4(u,m)\Phi_m(u)\sin mv,$$

$$M_v = -D\left[\frac{1}{u}\left(\frac{\partial u_z}{\partial u} + \frac{1}{u}\frac{\partial^2 u_z}{\partial v^2}\right) + \nu\frac{\partial^2 u_z}{\partial u^2}\right] =$$

$$= D\sum_{m=1}^{\infty}\left[\frac{1}{u}\left(\frac{d}{du} - \frac{m^2}{u}\right) + \nu\frac{d^2}{du^2}\right]\nabla^4(u,m)\Phi_m(u)\sin mv,$$

$$M_{uv} = -(1-\nu)\frac{D}{u}\frac{\partial}{\partial v}\left(\frac{\partial u_z}{\partial u} - \frac{u_z}{u}\right) =$$

$$= \mp(1-\nu)\frac{D}{u}\left(\frac{d}{du} - \frac{1}{u}\right)\sum_{m=1}^{\infty} m\nabla^4(u,m)\Phi_m(u)\sin mv.$$

where $\nabla_k^2(u,m)... = m\left(u\frac{d}{du} - 1\right)...$,

$$\nabla^2(u,m)... = \left(u^2\frac{d^2}{du^2} + u\frac{d}{du} - m^2\right)....$$

In order to find particular solution, it is possible to use Fourier series $\nabla^2(u,m)... = \left(u^2\frac{d^2}{du^2} + u\frac{d}{du} - m^2\right)...$, expand the right part of the equations (20) in trigonometric series:

$$-\frac{e^{4t}}{D}Z(t,v) = -\frac{e^{4t}}{D}\sum_{m=1}^{\infty} Z_m(t)\sin mv, \tag{27}$$

and obtain the solution m member of series

$$\left[\nabla^4\nabla^4(t,m) - p^2\nabla_k^2\nabla_k^2(t,m)\right]\overline{\Phi}(t) = -\frac{e^{4t}}{D}Z_m(t), \tag{28}$$

where $\nabla^4(t,m)...$ and $\nabla_k^2(t,m)...$ are the same as for a general solution

In the case of the loading applied only along Z axis, two cases can be considered: $Z_m = \frac{4q}{\pi m}$ for $0 < v < \pi$ or $Z_m = -\frac{4q}{\pi m}(-1)^{\frac{m+1}{2}}$ for $-\frac{\pi}{2} < v < \frac{\pi}{2}$, when $m =$ 1, 3, 5, …, and equation (28) can be rewritten as follows:

$$\begin{gathered}\left[\nabla^4\nabla^4(t,m) - p^2\nabla_k^2\nabla_k^2(t,m)\right]\overline{\Phi}(t) = -\frac{4q}{\pi m}\frac{e^{4t}}{D} \text{ for } 0 < v < \pi, \\ \left[\nabla^4\nabla^4(t,m) - p^2\nabla_k^2\nabla_k^2(t,m)\right]\overline{\Phi}(t) = \frac{4q}{\pi m}(-1)^{\frac{m+1}{2}}\frac{e^{4t}}{D} \text{ for } -\frac{\pi}{2} < v < \frac{\pi}{2},\end{gathered} \tag{29}$$

and finally

$$\begin{gathered}\overline{\Phi_m}(t) = Ae^{4t} \text{ for } 0 < v < \pi, \\ \overline{\Phi_m}(t) = -A(-1)^{\frac{m+1}{2}}e^{4t} \text{ for } -\frac{\pi}{2} < v < \frac{\pi}{2},\end{gathered} \tag{30}$$

where

$$A = \frac{-4q}{D\pi m\left[4^6 + m^8 - 40m^6 + 528m^4 - 2560m^2 - 9p^2m^2\right]}.$$

This method can be considered purely analythical, such solution became possible because of the simplicity of right helicoid quadratic forms. This solution results are precise and so that can be used as a benchmark for comparison to numeric and numeric-analythical solutions.

According to the methodology suggested in part 2.2, it is possible to analyze the stress-strain state of a shallow right helicoid. Several test examples are represented in comparison with results obtained by another methodology (part 2.1) for oblique helicoid in the case when the angle between the plane and the generator is equal to zero.

3. Results and Discussion

The numeric experiments were carried out in present investigation to verify and compare the methodologies given and also to define the border between shallow and non-shallow models.

The first comparison was made for method from chapter 2.1 and finite element method.

The comparison demonstrates close agreement of results, obtained by the numeric-analytic method and those obtained by finite element analysis.

The model is identic to model in example in 2.1.2.

The series of calculations were conducted for shells with different φ angle in limits from 0º to 15º.

Table 1. The results comparison for different angles.

φ	0	3	5	10	15
Maximum deflection along z axis method 1*, m	$8.69\cdot10^{-5}$	$8.45\cdot10^{-5}$	$8.43\cdot10^{-5}$	$7.99\cdot10^{-5}$	$4.67\cdot10^{-5}$
The same, method 2*, m	$8.7\cdot10^{-5}$	$8.6\cdot10^{-5}$	$8.0\cdot10^{-5}$	$7.4\cdot10^{-5}$	$6.6\cdot10^{-5}$
Maximum bending moment M_u, method 1*, KN·m/m	3914/ –1663	3805/ –1614	3593/ –1524	2853/ –1191	2076/ –852
The same, method 2*, KN·m/m	3711/ –1667	3689/ –1656	3639/ –1636	3428/ –1532	3108/ –1374

* method 1, – numeric- analytical, method 2 – finite element method

The finite element calculations were carried on by ANSYS APDL 15 software application. The finite element model represents a shell segment of 45º. It was proved that such a segment is sufficient to get the representative deflection and stress shape in the middle section [36]. The finite element SHELL181 was used for the calculation, quadrilateral finite elements were used according to the recommendations of official guideline [37], mesh size of 10 cm was sufficient to obtain the stable results. The loading was applied as gravity (dead load).

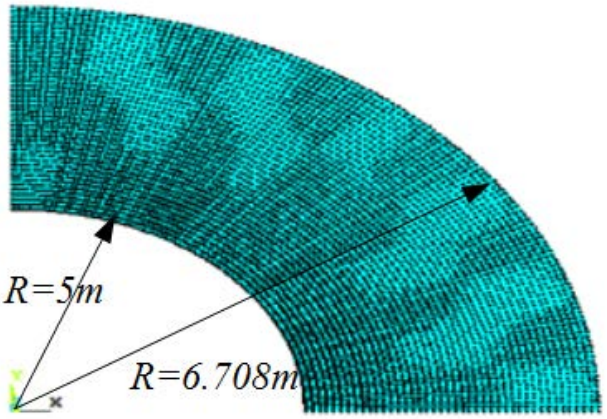

Figure 9. Finite element model.

Because of these results the boundary between shallow and non-shallow model can be determined near 10º generator obliquity angle for shells with a small pitch. This angle approximately corresponds to shell ratio of rise to plane size of 1/5.

The second comparison was made for right helicoid shell, calculated by numeric-analytic method and purely analytic method. The method from chapter 2.1 (for oblique helicoid) is also suitable for stress-strain analysis of shells with middle surface of special and degenerated cases of helicoid: if $\varphi = 0$ then oblique helicoid degenerates into right helicoid, if simultaneously $c = 0$ into flat plate; if $c = 0$, $\varphi \neq 0$ into conus. So we can compare results for right helicoid, calculated as a special case of oblique one, and analytically, directly as it was shown in chapter 2. Thus, the numeric-analythical methodology can be called

the handiest one, combining the advantages of analytical approach and universality of numeric Runge-Kutta solution.

The results obtained by the numeric-analytic method also have close agreement to those obtained by analytical method for right helicoid. The next examples illustrate this.

The shell of right helicoid form is analyzed below. The material characteristics: Young modulus E is $2 \cdot 10^5$ MPa, Poisson's ratio is 0.3. The thickness is 0.02 m, the inner radius R_1 is 5 m, the outer radius R_2 is 6.708 m, the pitch H = 0.314 m (or *c* = 0.05), load intensity is 10 KPa. All edges have fixed support.

The results are presented in the Fig. 10.

The maximum deflection is 1.51 mm, analytical method result is 1.48 mm.

The comparison with the results, got by analytical method is given in Table 2.

The results were obtained for analythical and numeric-analythical methodiques. First calculation was carried on for right helicoid as a special case of oblique helicoid by the numeric-analythical metodique, described in 1.1. The second one was conducted for the right helicod by the analytical methodique, described in 1.2. The graphs were plotted by means of free computer algebra system Giac/Xcas software. The result graphs are overaid on each other compare them visually.

The graphs from Fig. 9 (a-d) were obtained for the central section of long shell, remote enough from the fixed edge, that is considered by one-dimentional model of the corresponding methods The plots below illustrate that while deflection compared the difference between the values for 2 methodiques is about 0.03 mm, that means the discrepancy is about 2 % (Fig. 9 a). While bending moments M_u or shear forces Q_u compared, the difference is about 1 %, for it M_v is 2.5 %. All these results can be considered close or almost identical with technicall accuracy.

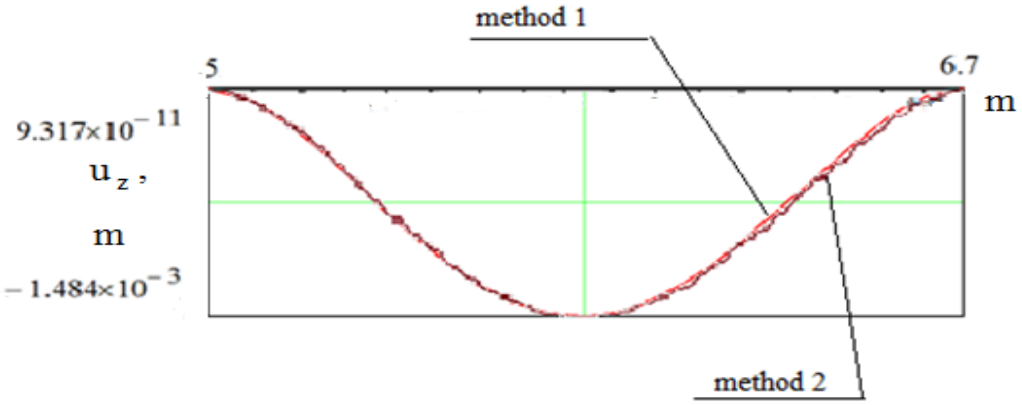

Figure 9 a. Deflection u_z

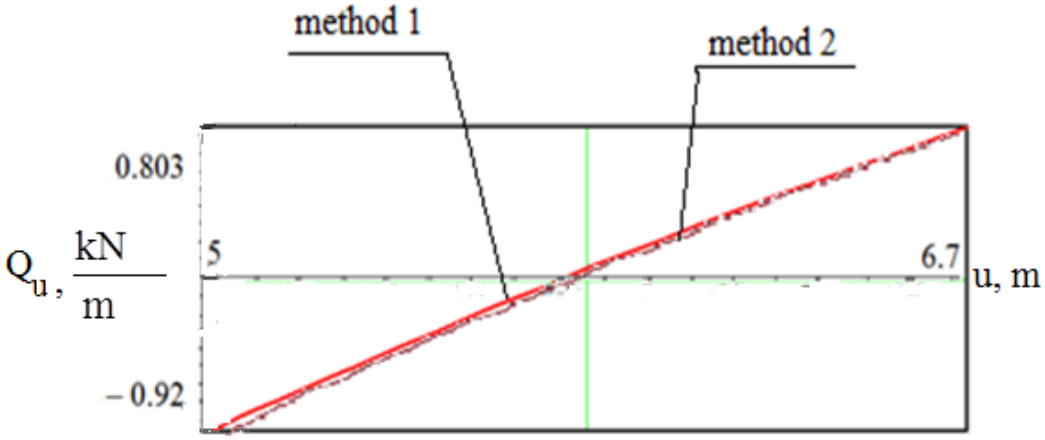

Figure 9 b. Shear force Q_u

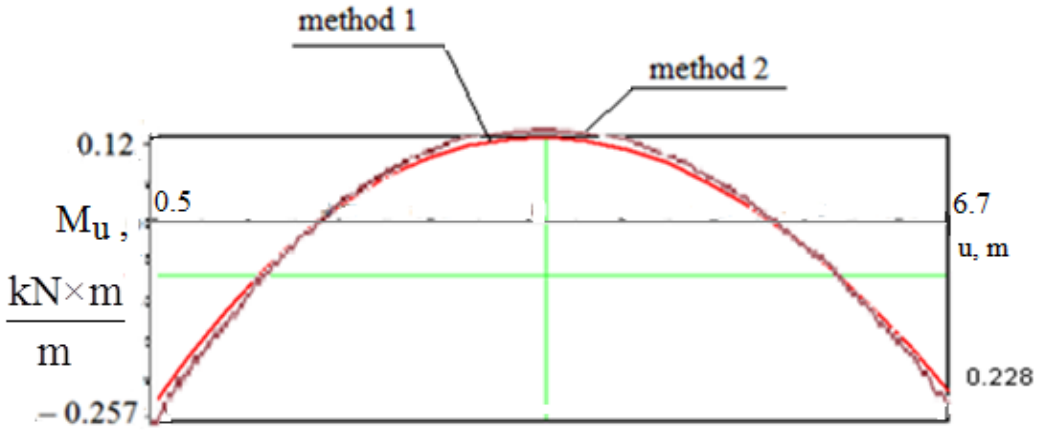

Figure 9 c. Bending moment M_u

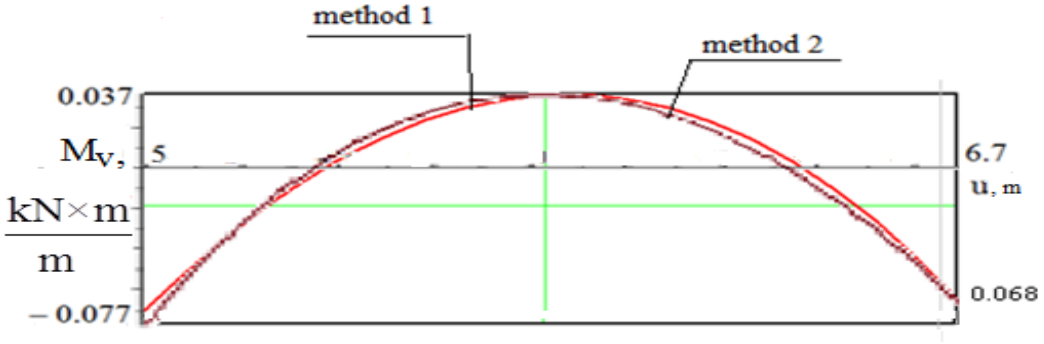

Figure 9 d. Bending moment M_v

All forces, moments and displacements except those which are represented on the graphs are close or equal to zero for shallow shells. These close matching results (see Table 2) show that the numeric-analythical methodology from 1.1 is more universal and can be used for any oblique helicoids including special cases, but the analythical methodology is certainly more accurate.

Table 2. The results comparison for two methods.

Quantity	Method 1	Method 2
Bending moment M_u, $\frac{kN\,m}{m}$ First support/midspan/second support	2,57/–1,21/2,289	2,57/–1,20/2,28
Bending moment M_v, $\frac{kN\,m}{m}$ First support/midspan/second support	0,77/–0,36/0,68	0,77/–0,37/0,68
Shear force kN First support/second support	–9,208/8,00	–9,208/8,03

Short finite element analysis was also conducted (see Fig. 11) by means of finite element software ANSYS APDL. The analogous calculation for another shell with different parameters was conducted in [38]. The finite element model is represented by one quarter of helicoid coil, because it is sufficient to neglects boundary effects [39]. The model is meshed by quadrilateral elements of 5 cm side length of 'shell 181' type, the element which behavoiur is based on Kirghoff-Love linear elastic model. This element size is sufficient for results convergence and appropriate accuracy of the calculation. The distributed load was applied, like own weight. All edges have fixed support. Finite element test also shows close agreement: deflection is 1.516 mm. The isofields of deflections are shown on Fig. 11. Only deflection were compared to avoid coordinate systems mismatch while comparing the inner force factors, because ANSYS has only Cartesian, cylindrical or spherical coordinates, but for corrects comparison curvilinear coordinates needed.

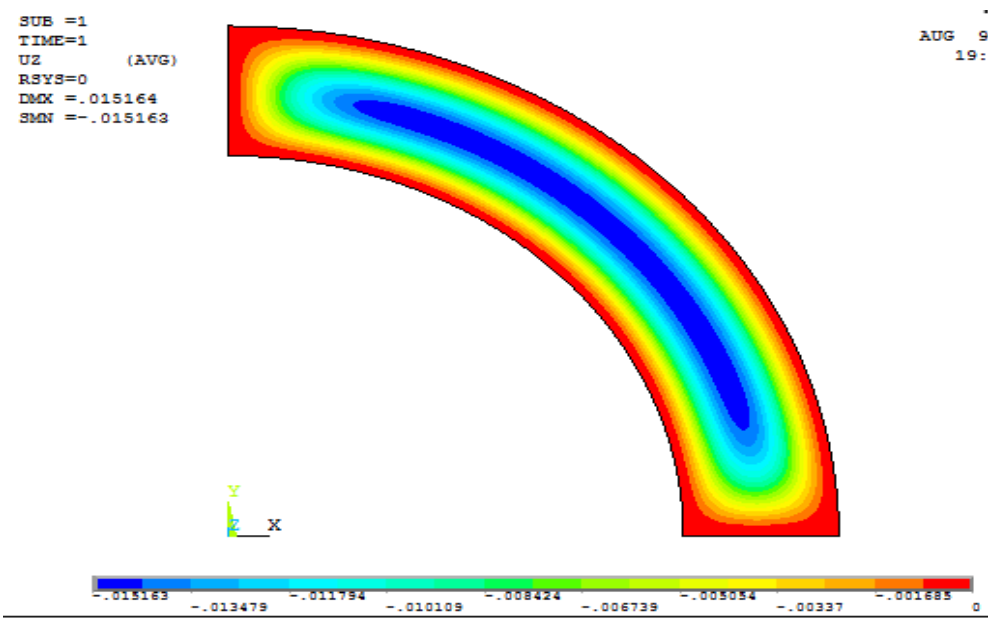

Figure 11. The deflection u_z by FE analysis.

4. Conclusion

In this paper two methodologies of analytical and half-analytical stress-strain state analysis for thin shallow helicoidal structures in the shape of right and oblique helicoids are represented. The analytical approach which is suitable for a right helicoid structure is compared to the half-analytical methodology which is developed by authors for an oblique helicoid structure when the inclination angle of generator is equal to zero (in this case the oblique helicoid turns into the right helicoid). The results which are obtained by two approaches give the appropriate accuracy if compared with each other, as well as if compared with the finite element method results.

The analytical approach for calculation of a right helicoidal structure is realized by the means of computer software based on analytical solutions obtained, while the half-analytical approach for calculation of an oblique helicoidal structure is performed by Giac/Xcas software. The finite element analysis was carried out by the means of Lira SAPR and ANSYS APDL software. The obtained results are also similar to the results obtained by analytical and numeric-analytical methods.

Both methodologies are written in the compact ways and are convenient for a practical engineering application as a means for a preliminary calculation or a deep stress-strain analysis of right and oblique helicoidal structures.

The boundary between shallow and non-shallow model was established approximately at 10^0 of generator obliquity, that corresponds to classical recommendations to apply shallow model when h/l (shell depth to span) ratio is less than 1/5.

All test calculations in this paper are made for cases with simple boundary conditions, mostly fixed supports (rigid restraints), because such cases need less computing time. In prospect this difficulty can be avoided with implementation of superior modifications of sweep method [40]. Another application of the methodology proposed is testing finite element model with the most simple load case and boundary conditions by comparison with the similar analytical model and following application of real loads on it.

To sum up, it may be said, that analytical methodology for right helicoid and numeric-analytic methodology for oblique and right helicoid have an advantages, as transparent physical meaning. The results are valid, the accuracy is appropriate, range of use is defined.

5. Acknowledgments

The paper has been supported by the RUDN University Strategic Academic Leadership Program.

6. Conflicts of Interest

The authors declare no conflict of interest.

References

1. Bradshaw, R., Campbell, D., Gargari, M., Mirmiran A., Tripeny, P. Special structures. Past, present, and future. Journal of Structural Engineering. 2002. 128 (6). Pp. 691–709. DOI: 10.1061/(ASCE)0733-9445(2002)128:6(691)
2. Adriaenssens, S., Block, P., Veennendaal, D., Williams, C. Shell Structures for Architecture – Form finding and Optimization, Routledge, 2014. 340 p. DOI: 10.4324/9781315849270
3. Fujimoto, K. House in Ashiya. Jutakutokushu. 2020. 1. Pp. 119–125.
4. Krivoshapko, S.N., Rynkovskaya, M., Razin, A. Design of a Thin Metal Product with the Developable Middle Surface from a Sheet by Parabolic Bending. Materials and Technologies in Engineering II, Materials Science Forum. 2020. 986. Pp. 78–85. DOI: 10.4028/www.scientific.net/MSF.986.78
5. Anisimov, R., Tarapanov, A. Design of the tool for periodic not evolvent profiles. MATEC Web of Conferences. 2017. 129 01039.
6. Abdullah, O.S., Khalil, W.H., Kamel, A.H., Shareef, A.J. Investigation of Physical and Numerical Model of Archimedes Screw Turbine. Journal of Power and Energy Engineering. 2020. 8. Pp. 26–42. https://doi.org/10.4236/jpee.2020.810003
7. Shahverdi, K., Loni, R., Ghobadian, B., Gohari, S., Marofi, S., Bellos, E. Numerical Optimization Study of Archimedes Screw Turbine (AST): A case study. Renew Energy. 145. Pp. 2130–2143. DOI: https://doi.org/10.1016/j.renene.2019.07.124
8. Nemirovskii, Yu.V., Babin, A.I., Sal'skii, E.A. Termonapryazhennoe sostoyanie mnogosloinykhpoliarmirovannykh gelikoidal'nykh obolochek [Thermo-stressed state of the helicoidalmultilayer polyreinforced shells]. Doklady Akademii nauk vysshei shkoly Rossiiskoi Federatsii – Proceedings of the Russian higher school Academy of sciences. 2016, 4 (33). Pp. 7–21. DOI: 10.17212/1727-2769-2016-4-7-21
9. Zhao, Y., Su, D., Wei, W., Dong, X. A meshing principle for generating a cylindrical gear using an Archimedes hob with two degrees of freedom. Proceedings of the Institution of Mechanical Engineers, Part C: Journal of Mechanical Engineering Science. 2010. 224 (1). Pp. 169–181. URL: https://doi.org/10.1243/09544062JMES1535
10. Akopyan, A.F., Akopyan, V.F., Podolko, K.Yu., Timoshenko, M.S., Boyarskikh, S.A., Litovchenko, T.A. Modelirovaniye raboty svay pri realizatsii prosadki grunta [Modeling of pile operation in the implementation of subsidence]. Inzhenernyy vestnik Dona. 2017. 3 (46). Pp. 92–95. URL: https://cyberleninka.ru/article/n/modelirovanie-raboty-svay-pri-realizatsii-prosadki-grunta
11. Smulskiy, I.I. Shnekovyye vetrodvigateli i ikh osobennosti [Screw wind turbines and their characteristics]. Inzhenerno-fizicheskiy zhurnal. 2001. 74(5). S. 187–195.
12. Jean Paul, V. A review of geometry investigations of helicoids. IOP Conference Series: Material Science Engineering. 2018. 371 012029. DOI: 10.1088/1757-899X/371/1/012029
13. Knabbel, J., Lewinski, T. Selected equilibrium problem of thin elastic helicoidal shells. Arch. Civil Eng. 1999. 42(2). Pp. 245–257.
14. Shevelev, L.P., Korikhin, N.V., Golovin, A.I. Sostoyaniya polya napryazheniy v gelikoidalnoy obolochke [Field stresses state in the helicoidal shell] Stroitelstvo unikalnykh zdaniy i sooruzheniy [Construction of Unique Buildings and Structures]. 2014. 2(17). S. 25–38. DOI: 10.18720/CUBS.17.2
15. Sorokina, A.G., Fomicheva, V.F., Kokoulin, V.G. Raschet napryazhenno-deformirovannogo sostoyaniya elastichnoy lenty gelikoidalnogo konveyera [Calculation of the stress-strain state of the elastic belt of a helical conveyor]. Inzhenernyy zhurnal: nauka i innovatsii. 2018. № 12 (84).
16. Savićević, S., Janjić, M., Vukčević, M., Šibalić, N. Stress research of helicoidal shell shape elements. Machines, technologies, materials, 2013, 10. URL: http://www.mech-ing.com/journal/Archive/2013/10/42_Savicevic_mtm13.pdf
17. Sorokina, A.G. Raschet formy deformirovannoy sredinnoy poverkhnosti gelikoidalno simmetrichnoy obolochki otkrytogo profilya pri bolshikh peremeshcheniyakh na osnove teorii chistogo izgibaniya [Calculation of the shape of the deformed median surface of a helicoidally symmetric shell of an open profile at large displacements based on the theory of pure bending]. Izvestiya vysshikh uchebnykh zavedeniy. Mashinostroyeniye. 2011. 11. S. 8–13.
18. Love, A.E.H. A treatise on the mathematical theory of elasticity I and II, Cambridge. 1927.
19. Evkin, A.Yu. Composite spherical shells at large deflections. Asymptotic analysis and applications, Composite Structures. 2020. 233 111577. DOI: 10.1016/j.compstruct.2019.111577
20. Zvereyaev, E.M. Saint-Venant – Picard – Banach Method for Integrating the Equations of the Theory of Elasticity of Thin-Walled Systems. PMM. 2019. 83(5–6). Pp. 823–833. (rus)
21. Valle, J.M., Martínez-Jiménez, P. Modified Bolle – Reissner Theory of Plates Including Transverse Shear Deformations. Latin American Journal of Solids and Structures. 2015. 12(2). Pp. 295–316. https://dx.doi.org/10.1590/1679-78251275
22. Michiels, T., Adriaenssens, S., Dejong, M. Form finding of corrugated shell structures for seismic design and validation using non-linear pushover analysis. Engineering Structures. 2019. 181. Pp. 362–373. URL: https://doi.org/10.1016/j.engstruct.20-18.12.043
23. Krivoshapko, S., Rynkovskaya, M. Five Types of Ruled Helical Surfaces for Helical Conveyers. Support Anchors and Screws. MATEC Web of Conferences. 2017. 95 06002
24. Rynkovskaya, M., Ivanov, V. Analytical Method to Analyze Right Helicoid Stress-Strain. Advanced Structured Materials. 2019. 92. Pp. 157–171. DOI: https://doi.org/10.1007/978-3-319-79005-3_11
25. Tupikova, E. Stress-strain analysis of the shells of the long oblique helicoid form. Journal of fundamental and applied science. 2017. 9(7S). Pp. 296–309. DOI: http://dx.doi.org/10.4314/jfas.v9i7s.28
26. Romanova, V.A., Rynkovskaya, M., Ivanov, V. Automatic Modeling of Surfaces with Identical Slopes. Advanced Structured Materials. 2019. 92. Pp.143–156. DOI: https://doi.org/10.1007/978-3-319-79005-3_10
27. Krivoshapko, S.N., Gbaguidi, A.G. Two methods of analysis of thin elasic open helicoidal shells. International Journal of Research and Reviews in Applied Sciences. 2012. 12(3). Pp. 382–390.
28. Krivoshapko, S.N. Geometry and strength of general helicoidal shells. Applied Mechanics Reviews. 1999. 52(5). Pp. 161–175.
29. Dekhtyar, A.S. Load carrying capacity of helicoidal shell. Structural Mechanics and Analysis of Constructions. 2013. 6. Pp. 1–6. (rus)
30. Abbena, E., Salamon, S., Gray, A. Modern differential geometry of curves and surfaces with Mathematica. CRC Press, 2017.
31. Zveryaev, E.M. Extraction of consistent shell theory equations from 3D theory of elasticity. Structural Mechanics of Engineering Constructions and Buildings, 2019.15(2). Pp.135–148. DOI: 10.22363/1815-5235-2019-15-2-135-148
32. Godunov, S.K. A method of orthogonal successive substitution for the solution of systems of difference equations. USSR Computational mathematics and mathematical physics. Nov. 1962. 2:6. Pp. 972–982.

33. Abramov, A.A. On the transfer of boundary conditions for systems of ordinary linear differential equations (A variant of the dispersive method). USSR Computational mathematics and mathematical physics. Mar. 1962. 1:3. Pp. 617–622.
34. Toro, E.F. Godunov methods: theory and applications. Springer Science+Business media. LLC, 2001.
35. Abramov, A.A. Numerical stability of a method of transferring boundary conditions. Computational Mathematics and Mathematical Physics. Mar. 2006. Vol. 46: 3. Pp. 382–387.
36. Krivoshapko, S.N. Static analysis of shells with developable middle surfaces. Applied Mechanics Reviews. 1998. 51. Pp. 731–746.
37. Kohnke, P. Ansys: Theory Reference, release 5.6, Ansys, inc. 1999.
38. Tupikova, E.M. Raschet tonkikh uprugikh obolochek v forme dlinnogo kosogo gelikoida. Stroitelnaya mekhanika inzhenernykh konstruktsiy i sooruzheniy [Analysis of thin elastic shells in the form of thin oblique helicoid]. 2015. № 3. Pp. 23–27.
39. Aleksandrov, A.V., Kositsyn, S.B., Kositsyn, A.S. Netraditsionnyye modeli konechnykh elementov vysokikh poryadkov [Unconventional high-order finite element models]. Teoreticheskiye osnovy stroitelstva. Warszawa 2.07.96-5.07.96. Moskva: Izd-vo ASV, 1996. Pp. 26–30.
40. Vinogradov, A.Yu. Numerical modeling of boundary conditions in deformation problems of structured material in thin wall constructions. International Symposium Advances in Structured and Heterogeneous Continua II. Moscow, Russia, Book Abstracts. Aug. 1995.

Contacts:

Evgeniya Tupikova, emelian-off@yandex.ru
Marina Rynkovskaya, marine_step@mail.ru